⌘ *Author's Choice*

THE JOURNAL OF BIOLOGICAL CHEMISTRY VOL. 287, NO. 4, pp. 2558–2567, January 20, 2012

Dissociation of Inositol-requiring Enzyme (IRE1α)-mediated c-Jun N-terminal Kinase Activation from Hepatic Insulin Resistance in Conditional X-box-binding Protein-1 (XBP1) Knock-out Mice*[S]

Received for publication, October 24, 2011, and in revised form, November 22, 2011 Published, JBC Papers in Press, November 28, 2011, DOI 10.1074/jbc.M111.316760

Michael J. Jurczak[‡], Ann-Hwee Lee[§], Francois R. Jornayvaz[¶], Hui-Young Lee[‡], Andreas L. Birkenfeld[¶], Blas A. Guigni[¶], Mario Kahn[¶], Varman T. Samuel[¶], Laurie H. Glimcher[§‖], and Gerald I. Shulman[‡¶1]**

*From the [‡]Howard Hughes Medical Institute and Departments of [¶]Internal Medicine and **Cellular & Molecular Physiology, Yale University School of Medicine, New Haven, Connecticut 06536-8012 and the Departments of [§]Immunology and Infectious Diseases and [‖]Medicine, Harvard Medical School, Boston, Massachusetts 02115*

Background: Endoplasmic reticulum (ER) stress has been implicated in causing hepatic insulin resistance.
Results: Fructose-fed XBP1 knock-out mice were protected from hepatic insulin resistance despite increased hepatic ER stress and JNK activation.
Conclusion: ER stress and hepatic JNK activation can be disassociated from hepatic insulin resistance.
Significance: Hepatic ER stress is not a direct causal factor in hepatic insulin resistance.

Hepatic insulin resistance has been attributed to both increased endoplasmic reticulum (ER) stress and accumulation of intracellular lipids, specifically diacylglycerol (DAG). The ER stress response protein, X-box-binding protein-1 (XBP1), was recently shown to regulate hepatic lipogenesis, suggesting that hepatic insulin resistance in models of ER stress may result from defective lipid storage, as opposed to ER-specific stress signals. Studies were designed to dissociate liver lipid accumulation and activation of ER stress signaling pathways, which would allow us to delineate the individual contributions of ER stress and hepatic lipid content to the pathogenesis of hepatic insulin resistance. Conditional XBP1 knock-out (XBP1Δ) and control mice were fed fructose chow for 1 week. Determinants of whole-body energy balance, weight, and composition were determined. Hepatic lipids including triglyceride, DAGs, and ceramide were measured, alongside markers of ER stress. Whole-body and tissue-specific insulin sensitivity were determined by hyperinsulinemic-euglycemic clamp studies. Hepatic ER stress signaling was increased in fructose chow-fed XBP1Δ mice as reflected by increased phosphorylated eIF2α, *HSPA5* mRNA, and a 2-fold increase in hepatic JNK activity. Despite JNK activation, XBP1Δ displayed increased hepatic insulin sensitivity during hyperinsulinemic-euglycemic clamp studies, which was associated with increased insulin-stimulated IRS2 tyrosine phosphorylation, reduced hepatic DAG content, and reduced PKCε activity. These studies demonstrate that ER stress and IRE1α-mediated JNK activation can be disassociated from hepatic insulin resistance and support the hypothesis that hepatic insulin resistance in models of ER stress may be secondary to ER stress modulation of hepatic lipogenesis.

Post-prandial hyperglycemia is a key feature of type 2 diabetes and arises, in part, from the inability of insulin to properly suppress hepatic glucose production because of hepatic insulin resistance (1). The pathogenesis of hepatic insulin resistance is incompletely understood, and both accumulation of intracellular lipids (*e.g.* diacylglycerol, ceramides, etc.) and excessive endoplasmic reticulum (ER)[2] stress have been proposed to be responsible (2–4). Reducing ER stress pharmacologically improves hepatic insulin sensitivity (5–7); however, such interventions also decrease hepatic steatosis, raising the possibility that changes in hepatic insulin sensitivity result from reduced intracellular lipid levels and not directly from improvements in ER stress signaling pathways.

The X-box-binding protein-1 (XBP1) is a transcriptional regulator of the ER stress response that lies downstream of inositol-requiring enzyme 1 (IRE1α) activation (8). IRE1α possesses both kinase and ribonuclease activity and processes XBP1 mRNA to produce an active transcription factor in response to ER stress (9, 10). Homozygous deletion of XBP1 results in embryonic lethality, and heterozygous XBP1 null mice are prone to ER stress and high-fat diet-induced insulin resistance, resulting from IRE1α-mediated JNK activation, although

* This work was supported by United States Public Health Service Grants R01 DK-40936, P30 DK-45735, U24 DK-059635, and DK-082448 (to L. H. G.), the American Heart Foundation (to A.-H. L.), Swiss National Science Foundation Grant PASMP3-132563 (to F. R. J.), and German Research Science Foundation Grant Bi1292/4-1 (to A. L. B.).
⌘ *Author's Choice*—Final version full access.
[S] This article contains supplemental Fig. S1.
[1] To whom correspondence should be addressed: Howard Hughes Medical Institute, Yale University School of Medicine, TAC S269, P.O. Box 9812, New Haven, CT06536-8012. Tel.: 203-785-5447; Fax: 203-737-4059; E-mail: gerald.shulman@yale.edu.

[2] The abbreviations used are: ER, endoplasmic reticulum; DAG, diacylglycerol; DGAT2, diacylglycerol *o*-acyltransferase 2; FASN, fatty acid synthase; FoxO1, forkhead box O1; G6PC, glucose-6-phosphatase; GPAT1, glycerol-3-phosphate acyl transferase 1; GRP78, 78-kDa glucose-regulated protein; HSPA5, heat shock protein 5; IRS, insulin receptor substrate; LCCoA, long-chain CoA; PEPCK, phosphoenolpyruvate carboxykinase; SCD1, sterol CoA desaturase 1; SPT, serine palmitoyl transferase; SREBP, sterol regulatory element-binding protein.

hepatic lipid levels were not determined (5). Recently, conditional deletion of XBP1 (XBP1Δ) in mice was found to reduce plasma lipid levels as a result of decreased hepatic lipogenesis, with no effect on liver lipid content (11). Interestingly, XBP1Δ mice displayed increased activation of the IRE1α arm of the ER stress response (11).

Because hepatic lipid content, ER stress, and inflammation are all increased under high-fat diet conditions, it is difficult to delineate the relative contribution of each of these mechanisms to the pathogenesis of hepatic insulin resistance. We therefore elected to challenge XBP1Δ mice with a fructose chow diet to assess the respective roles of ER stress and liver lipids in the development of hepatic insulin resistance. We reasoned that because XBP1Δ mice display reduced hepatic lipogenesis (11), fructose feeding would allow us to delineate the individual contributions of ER stress and hepatic lipid content to the pathogenesis of hepatic insulin resistance.

EXPERIMENTAL PROCEDURES

Animal Use and Care—XBP1Δ mice were generated as previously described (11). Briefly, XBP1^{flox} mice with loxP sites flanking exon 2 of the *XBP1* gene were backcrossed with Mx1-cre mice that express interferon-dependent cre recombinase. The mice were backcrossed for more than five generations onto the C57BL/6 background. Injection of mice one to three times with 250 μg of poly(I:C) at 2-day intervals results in cre-mediated deletion of exon 2 and introduction of a translational termination codon because of a reading frameshift. Quantitative PCR with primers specific to exon 2 (XBP205, CCTGAGCCCGGAGGAGAA; XBP272, CTCGAGCAGTCTGCGCTG) of the *XBP1* gene was used to confirm cre-mediated deletion of XBP1. The mice were housed at Yale University School of Medicine and maintained in accordance with the Institutional Animal Care and Use Committee guidelines. The mice were housed at 22 ± 2 °C on a 12-h light, 12-h dark cycle with free access to food and water. The mice were fed 1 week of fructose chow diet in pellet form (13% fat, 67% carbohydrate, 20% protein by calories; carbohydrate source: 100% fructose; fat source: 100% lard; protein source: 100% casein + DL-methionine supplement; mineral mix: Rogers-Harper 170760; vitamin mix: Teklad 40060 TD89247; Harlan Teklad) and studied at 14–16 weeks of age. Body composition was determined by ^{1}H magnetic resonance spectroscopy (Bruker Minispec). The comprehensive lab animal monitoring system (Columbus Instruments, Columbus, OH) was used to evaluate activity, energy expenditure, feeding, drinking, and respiratory quotient over the course of 48 h. The data are the 24-h averages normalized to body weight.

Quantitative PCR, Western Blotting, and Activity Assays—RNA from adipose and liver was isolated using an RNeasy kit (Qiagen) according to the manufacturer's instructions and then used for cDNA synthesis using a reverse transcriptase PCR kit (Qiagen). Quantitative PCR was performed with the Applied Biosytems 7500 Fast RT-PCR system and SYBR Green detection reagent. Primer sequences for transcripts of proteins involved in lipid and glucose metabolism were designed with Primer Express Software (Applied Biosytems) and were as follows: ACC2 (acetyl CoA carboxylase 2), forward TGTGGACGTTGAATTGATTTACG and reverse GCCGGTGGGCATCGAT; DGAT2, forward TGGGCCTTGGTGGTTTCTTAC and reverse GACTGCCCTTGCCCAGCTA; FASN, forward CAAGCAGAATTTGTCCACCTTTAA and reverse TCTCTAGAGGGCTTGCACCAA; SCD1, forward TGCCCCTGCGGATCTTC and reverse GGCCCATTCGTACACGTCAT; PEPCK, forward GTCACCATCACTTCCTGGAAGA and reverse GGTGCAGAATCGCGAGTTG; G6PC, forward GTGGCAGTGGTCGGAGACT and reverse ACGGGCGTTGTCCAAAC; GPAT1, forward GGCGAGAGGCGTTATCAGAA and reverse AGGAAAATGGCTGTGCAAAATC; and SPT, forward CAAGGCCAGAAGGCTTATGTG and reverse TTTGGTGAGCAGAACAGAAAGAGA. The expression of genes involved in the ER stress response was quantified using SA Biosciences designed PCR primers according to the manufacturer's instructions.

The tissues were homogenized in radioimmune precipitation assay buffer (150 mM NaCl, 1% (v/v) Triton X-100, 0.1% (w/v) SDS, 0.5% (w/v) sodium deoxycholate, 50 mM Tris-HCl) supplemented with protease inhibitors (Pierce) and EDTA for protein extraction. Protein concentration was determined using Bradford reagent, and equal protein (50 μg) was loaded for Western blotting. For immunoprecipitations, the lysates were diluted, and 1 mg of total protein was incubated overnight at the suggested dilution with primary antibody for the protein of interest. Cytoplasmic and nuclear fractionation was performed with the NE-PER kit (Pierce). PKCϵ activity was determined as previously described (12). JNK activity was measured in whole cell lysates as well as cytoplasmic and nuclear fractions with a JNK/SAPK activity assay (Cell Signaling, Danvers, MA) according to the manufacturer's instructions. Sources of antibodies: Cell Signaling: IRE1α, JNK, GRP78, phosphorylated Tyr, phosphorylated IRS1 (Ser-307), and phosphorylated and total eIF2α; Millipore (Billerica, MA): IRS1 and IRS2; and Santa Cruz (Santa Cruz, CA): GAPDH.

Hepatic Metabolite Analyses—Hepatic triglycerides were extracted using a methanol/chloroform-based method (12) and quantified with a colorimetric kit (Genzyme, Cambridge, MA), and diacylglycerol, ceramide, and long chain acycl CoA (LCCoA) levels were measured as previously described (12–14). Post-clamp liver glycogen levels were determined as previously described (13) following precipitation on glass filters and release of glucose by amyloglucosidase digestion.

Hyperinsulinemic Euglycemic Clamp Study—Clamps were performed according to recent recommendations of the Mouse Metabolic Phenotyping Center Consortium (15). After surgical implantation of an indwelling catheter in the right jugular vein, the mice were allowed to recover for 1 week prior to clamp experiments. Following an overnight 14-h fast, the mice were infused with 3-[^{3}H]glucose at a rate of 0.05 μCi/min for 120 min to determine basal glucose turnover. Next, a primed infusion of insulin and 3-[^{3}H]glucose was administered at 7.14 milliunits·kg^{-1}·min^{-1} and 0.24 μCi/min, respectively, for 4 min, after which the rates were reduced to 3 milliunits·kg^{-1}·min^{-1} insulin and 0.1 μCi/min 3-[^{3}H]glucose for the remainder of the experiment. Blood was collected via tail massage for plasma glucose, insulin, and tracer levels at set time points during the 140-min infusion, and a

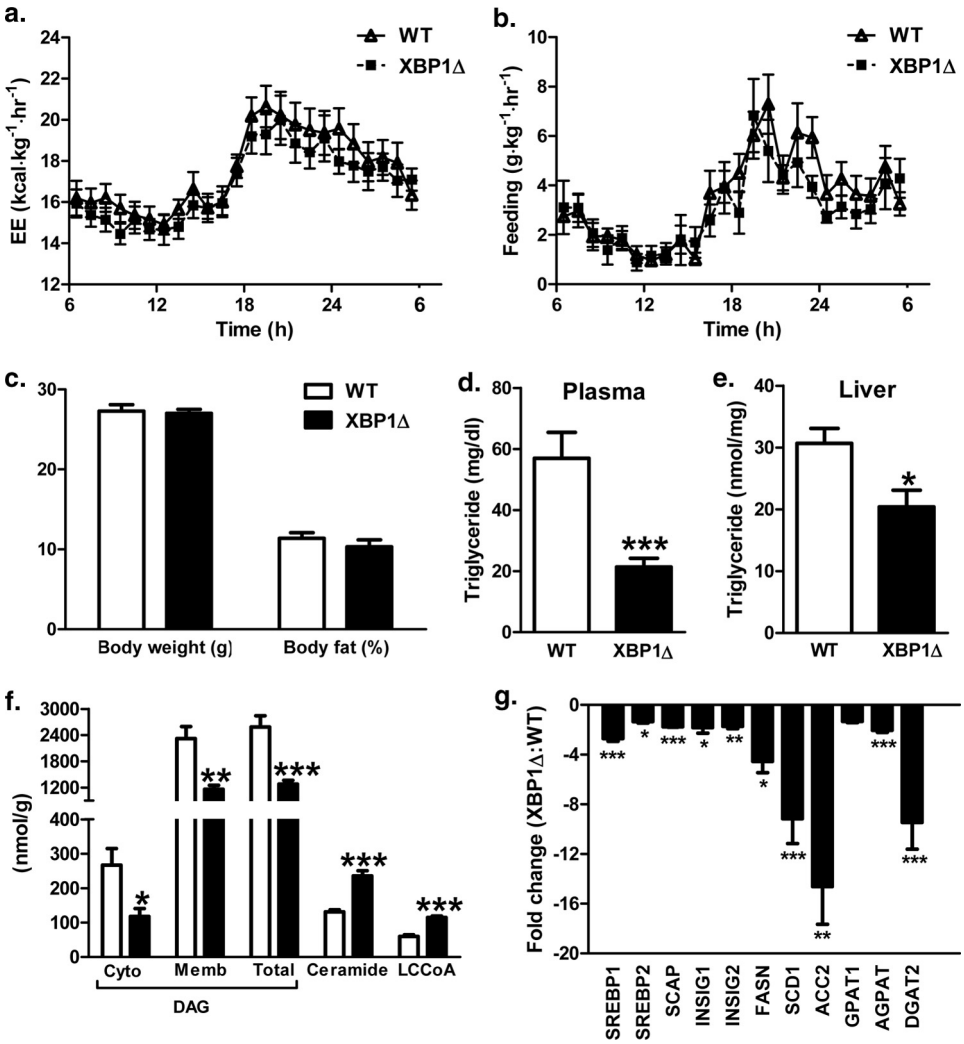

FIGURE 1. **XBP1Δ mice fed fructose chow have reduced hepatic lipid levels and expression of lipogenic genes.** *a*, 24-h energy expenditure (*EE*) during fructose chow feeding. *b*, 24-h feeding during fructose feeding. *c*, body weight and fat mass after 1 week of fructose feeding. *d*, plasma triglyceride levels. *e*, hepatic triglyceride levels. *f*, hepatic DAG levels in cytosol (*Cyto*) and membrane (Memb) compartments, and ceramide and LCCoA levels. *g*, quantitative PCR of cDNA from liver of genes involved in lipid metabolism. The data are expressed as fold change relative to WT. ($n = 6–8$ for both genotypes aged 14–16 weeks for each panel). *, $p < 0.05$; **, $p < 0.001$; ***, $p < 0.001$.

variable infusion of 20% dextrose was given to maintain euglycemia. Glucose turnover was calculated as the ratio of the 3-[^{3}H]glucose infusion rate to the specific activity of plasma glucose at the end of the basal infusion and during the last 40 min of the hyperinsulinemic-euglycemic clamp study. Hepatic glucose production represents the difference between the glucose infusion rate and the rate of glucose appearance. A 10-μCi bolus injection of [^{14}C]2-deoxyglucose was given at 90 min to determine tissue-specific glucose uptake, which was calculated from the area under the curve of [^{14}C]2-deoxyglucose detected in plasma and the tissue content of [^{14}C]2-deoxyglucose-6-phosphate, as previously described (16). Following collection of the final blood sample, the mice were anesthetized with an intravenous injection of 150 mg/kg pentobarbital, and tissues were harvested and froze with aluminum forceps in liquid nitrogen. All of the tissues were stored at −80 °C until later use.

Biochemical Analyses—Plasma glucose concentrations were measured by a glucose oxidase method using a Beckman Glucose Analyzer II. Plasma insulin was measured by radioimmunoassay kit (Linco Research, St. Louis, MO), and fatty acids were measured by a spectrophotometric technique (Wako NEFA Kit, Osaka, Japan). Plasma cytokines were measured by electrochemiluminescence detection on the Meso Scale Discovery® platform.

Statistical Analysis—The data are reported as the means ± S.E. Comparisons between groups were made using two-tailed, unpaired Student's *t* tests. A *p* value of less than 0.05 was considered significant. Statistical analyses were performed using GraphPad Prism 5.

RESULTS

XBP1Δ Mice Display Reduced Hepatic Lipid Levels and Increased JNK Activity after Fructose Chow Intervention—Because hepatic lipid levels and markers of ER stress are similar in regular chow-fed XBP1Δ and WT mice (11) and two additional mouse models of XBP1 deficiency have reported no changes in hepatic ER stress or insulin sensitivity under regular chow conditions (5, 17), we elected to study fructose-fed animals. During 1 week of fructose diet intervention, there was no difference in feeding or energy expenditure between body weight-matched

WT and XBP1Δ mice (Fig. 1, *a* and *b*). Also, the respiratory quotient was not different between groups (dark cycle: WT 0.956 ± 0.010, XBP1Δ 0.949 ± 0.007; $p = 0.61$; light cycle: WT 0.886 ± 0.008, XBP1Δ 0.896 ± 0.012; $p = 0.49$; 24-h average: WT 0.917 ± 0.008, XBP1Δ 0.920 ± 0.009; $p = 0.83$). Accordingly, there were no detectable changes in body weight or fat mass between genotypes after 1 week of fructose chow feeding (Fig. 1*c*). Plasma triglyceride levels were 60% lower in XBP1Δ mice (Fig. 1*d*), and hepatic triglyceride levels were significantly reduced (Fig. 1*e*). Interestingly, total hepatic diacylglyercol (DAG) content, which is associated with hepatic insulin resistance in several rodent models (2, 18–27), was reduced by 50% in XBP1Δ mice. Notably, both membrane and cytosolic levels of DAGs were significantly reduced. Hepatic ceramide content, which is also associated with hepatic insulin resistance in some (4) but not all models (28), as well as LCCoA levels, were increased by ~2-fold in the XBP1Δ mice compared with the WT mice (Fig. 1*f*). We confirmed reduced SREBP1 mRNA levels in fructose chow-fed XBP1Δ mice (11) and also found a reduction in SREBP2 and genes encoding the regulatory proteins SCAP (SREBP cleavage-activating protein), INSIG1, and INSIG2 (insulin-induced genes), which are required for SREBP1 and SREBP2 activation (Fig. 1*f*). More dramatic reductions ranging from 4- to 14-fold were detected for the lipogenic regulators FASN, SCD1, and ACC2 (Fig. 1*f*), which may account for reductions in lipogenesis and hepatic lipid content. Interestingly, there was a modest reduction in GPAT1 expression ($p = 0.15$) and more significant reductions of 2- and 8-fold for acylglycerol-3-phosphate acyltransferase and DGAT2 expression in XBP1Δ liver (Fig. 1*g*), whereas SPT mRNA was moderately increased (1.3 ± 0.1-fold increase, $p = 0.07$). Because DAGs and triglycerides are synthesized from LCCoAs by the sequential activity of GPAT, acylglycerol-3-phosphate acyltransferase, and DGAT enzymes and ceramide derives from LCCoAs entering the sphingolipid biosynthetic pathway via SPT, these changes may account for the observed differences in LCCoA, DAG/triglyceride, and ceramide levels.

Next, we examined the impact of fructose feeding on hepatic ER function in the absence of XBP1. Fructose chow-fed XBP1Δ mice displayed marked increases in IRE1α protein levels (Fig. 2*a*), consistent with previous observations in mice fed regular chow (11). IRE1α has been implicated in the ER stress-mediated activation of JNK (29) and subsequent serine phosphorylation of IRS1, resulting in hepatic insulin resistance (5, 30, 31). Activation of the protein kinase R-like ER kinase branch of the ER stress response was also evident because phosphorylated eIF2α levels were increased in XBP1Δ mice (Fig. 2*a*). Consistent with eIF2α activation, hepatic ATF4 mRNA showed a tendency to be increased in the XBP1Δ mice (Fig. 2*b*; $p = 0.09$). Genes involved in ER protein folding, binding, and glycosylation were up-regulated in fructose chow-fed XBP1Δ mice, including heat shock protein 5 (*HSPA5*), heat shock protein 4 (*HSPA4*), and UDP-glucose glycoprotein glucosyltransferase 2 (*UGGT2*). *ERN1*, encoding IRE1α, was also 2-fold greater in XBP1Δ mice, consistent with increased protein levels (Fig. 2*a*). Protein levels of the *HSPA5* gene product GRP78 were also increased in XBP1Δ mice (Fig. 2*c*), consistent with changes in mRNA. Interestingly, XBP1-dependent ER stress response genes *EDEM* (an ER degradation enhancer) and *DNAJB9* (a Dnaj homolog) were significantly lower in XBP1Δ mice (Fig. 2*b*), supporting the observation that loss of normal fructose chow-induced activation of XBP1 results in blunted induction of XBP1 target genes (11). *RPN1* and *SIL1*, additional XBP1 targets (32, 33), were also decreased in XBP1Δ mice (Fig. 2*c*). Lastly, *PPP1R15B* , which encodes the protein CReP (constitutive repressor of eIF2α phosphorylation) and regulates protein phosphatase-1 mediated desphosphorylation of eIF2α, was 2.3-fold lower in the XBP1Δ mice (Fig. 2*b*) and may have contributed to the observed differences in phosphorylated eIF2α (Fig. 2*a*), suggesting the presence of a novel negative regulatory feedback loop between the IRE1α and protein kinase R-like ER kinase branches of the ER stress response.

IRE1α activation is responsible for ER stress-mediated activation of JNK, and increased IRE1α protein levels alone are sufficient for JNK activation (29). Here, we found increased IRE1α protein levels were associated with a 2-fold increase in JNK activity, measured by solid phase protein kinase assay (5, 34), in fructose chow-fed XBP1Δ mice (Fig. 2*d*). Because cellular localization of JNK activity has been shown to impact its contribution to insulin resistance (35), we measured JNK activity in cytosolic and nuclear fractions of liver cells. JNK activity was significantly greater in the XBP1Δ mice in the cytosolic fraction, whereas there was no difference in nuclear activity (Fig. 2*d*). The fold increase in cytosolic activity was not as robust as what was measured in whole cell lysates and may reflect a loss of activity during cellular fractionation. TNFα and IL1β are known to activate JNK (36); however, plasma TNFα levels were below the level of detection (2.5 pg/ml), and there was no difference in IL1-β between groups (Fig. 2*e*). Plasma IFNγ levels were also below the level of detection, and no differences in plasma concentrations of IL-6, IL-10, or IL-12 were detected (Fig. 2*e*).

Hepatic Insulin Sensitivity Is Improved in XBP1Δ Mice following Fructose Chow Intervention—To evaluate the impact of decreased liver lipids and increased JNK activity on hepatic insulin sensitivity, fructose chow-fed XBP1Δ and WT mice were subjected to hyperinsulinemic-euglycemic clamp studies. After overnight fast, plasma glucose levels were 25% lower in XBP1Δ mice compared with WT (Fig. 3*a*). Decreased fasting plasma glucose levels were associated with a 25% reduction in basal hepatic glucose production (Fig. 3*c*) and a 30% reduction in fasting plasma insulin concentrations (Fig. 3*b*). During hyperinsulinemic-euglycemic clamp, the glucose infusion rate required to maintain euglycemia was 1.5-fold greater for XBP1Δ mice (Fig. 3*d*), demonstrating a 50% improvement in whole-body insulin sensitivity (Fig. 3*e*). Importantly, there was no difference in post-clamp plasma insulin levels (WT, 48.0 ± 6.2 microunits/ml; XBP1Δ, 52.1 ± 3.9 microunits/ml; $p = 0.58$). The difference in whole-body insulin sensitivity was attributed to increased hepatic-insulin responsiveness, as reflected by a 80% suppression of hepatic glucose production during the hyperinsulinemic-euglycemic clamp in the XBP1Δ mice compared with only 30% suppression in the WT mice (Fig. 3*c*). There was no difference in whole-body glucose disposal (Fig. 3*f*). Consistent with these findings, post-clamp hepatic glyco-

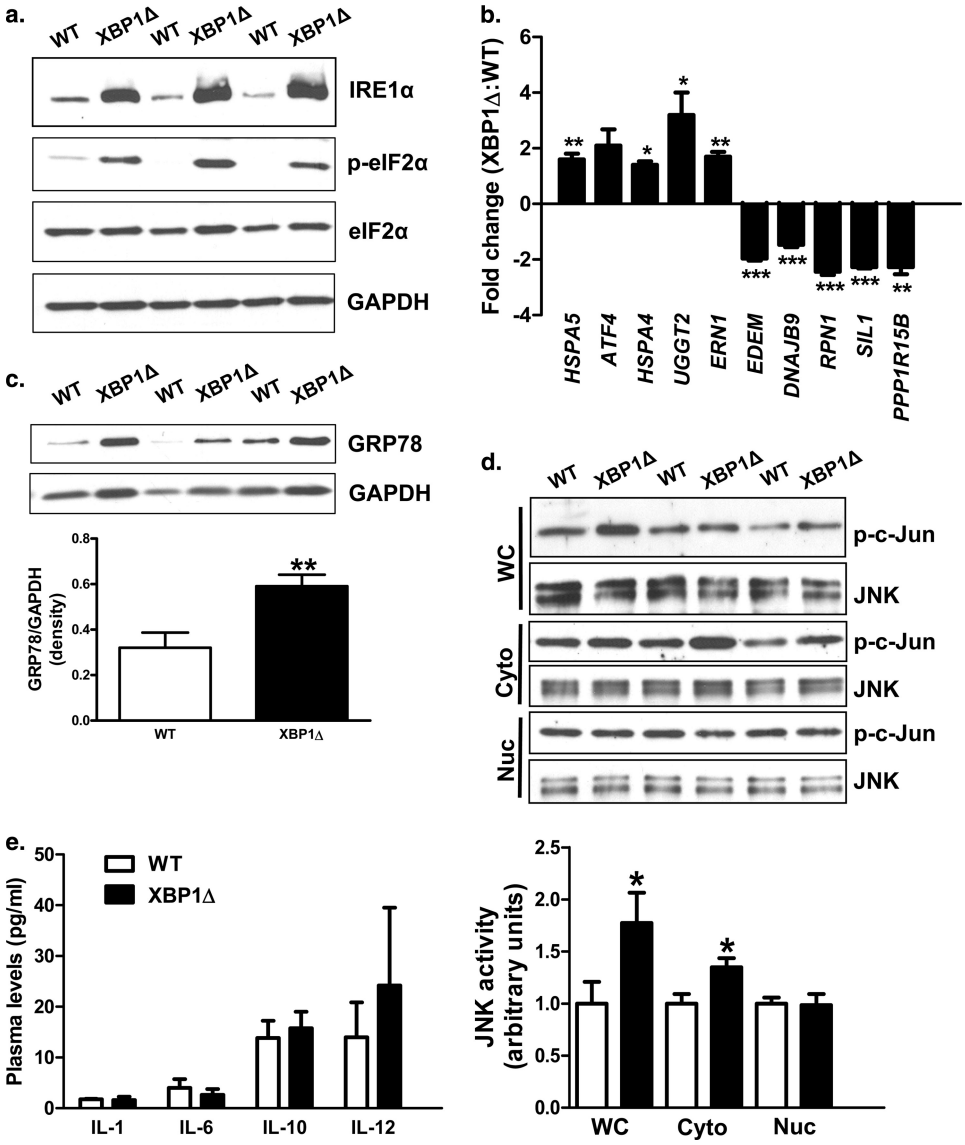

FIGURE 2. **Markers of ER stress are elevated in fructose chow-fed XBP1Δ mice.** *a*, Western blots of liver lysates for ER stress markers IRE1α, phosphorylated and total eIF2α, and GAPDH loading control. *b*, quantitative PCR of cDNA isolated from liver for genes involved in the ER stress response. The data are reported as fold change relative to WT. *c*, Western blot of liver lysate for the ER chaperone GRP78 and GAPDH loading control. *d*, hepatic JNK activity from whole cell liver lysates (*WC*), cytoplasmic (*Cyto*), and nuclear (*Nuc*) fractions obtained by differential centrifugation. *e*, plasma levels of the cytokines IL1-β, IL-6, IL-10, and IL-12. TNFα and INFγ were below the level of detection (2.5 pg/ml) ($n = 6–8$ for both genotypes for each panel). The blots shown are representative of six to eight mice per genotype. *, $p < 0.05$; **, $p < 0.001$; ***, $p < 0.001$.

gen content was markedly increased in the XBP1Δ mice (Fig. 3*g*).

Whole-body heterozygous XBP1 knock-out mice are prone to ER stress and display impaired insulin signaling in liver and adipose tissue during high fat diet feeding (5). During the euglycemic clamp, infusion with [^{14}C]2-deoxyglucose demonstrated no difference in adipose tissue-specific glucose uptake in fructose-fed XBP1Δ mice compared with WT (supplemental Fig. S1*a*). *XBP1* deletion in XBP1Δ adipose tissue in response to poly(I:C) injection was modest compared with liver and was not significant (supplemental Fig. S1*b*; $p = 0.15$). Accordingly, there was no difference in SCD1, ACC2, DGAT2, or FASN gene expression in adipose tissue of XBP1Δ compared with WT mice (supplemental Fig. S1*b*). Also, phosphorylated eIF2α levels did not differ between genotypes, and IRE1α protein levels were inconsistently elevated in XBP1Δ mice and correlated with a degree of XBP1 knock-out (supplemental Fig. S1*c*).

Improved Hepatic Insulin Sensitivity Is Associated with Changes in Hepatic Insulin Signaling in XBP1Δ Mice following Fructose Challenge—JNK can phosphorylate serine 307 of IRS1 *in vitro*, reducing tyrosine phosphorylation and impairing insulin signaling, and phosphorylation of IRS1 serine 307 is a commonly reported feature in models of hepatic insulin resistance (37, 38). In contrast, IRS1 tyrosine phosphorylation trended to be increased in XBP1Δ mice, despite JNK activation (Fig. 4, *a* and *b*; $p = 0.10$). Total levels of IRS1 serine 307 phosphorylation were low, and no differences were observed between genotypes in IRS1 immunoprecipitated samples (Fig. 4, *a* and *b*) or in whole cell lysates (data not shown). IRS1 serine phosphorylation under insulin-stimulated conditions represents only a

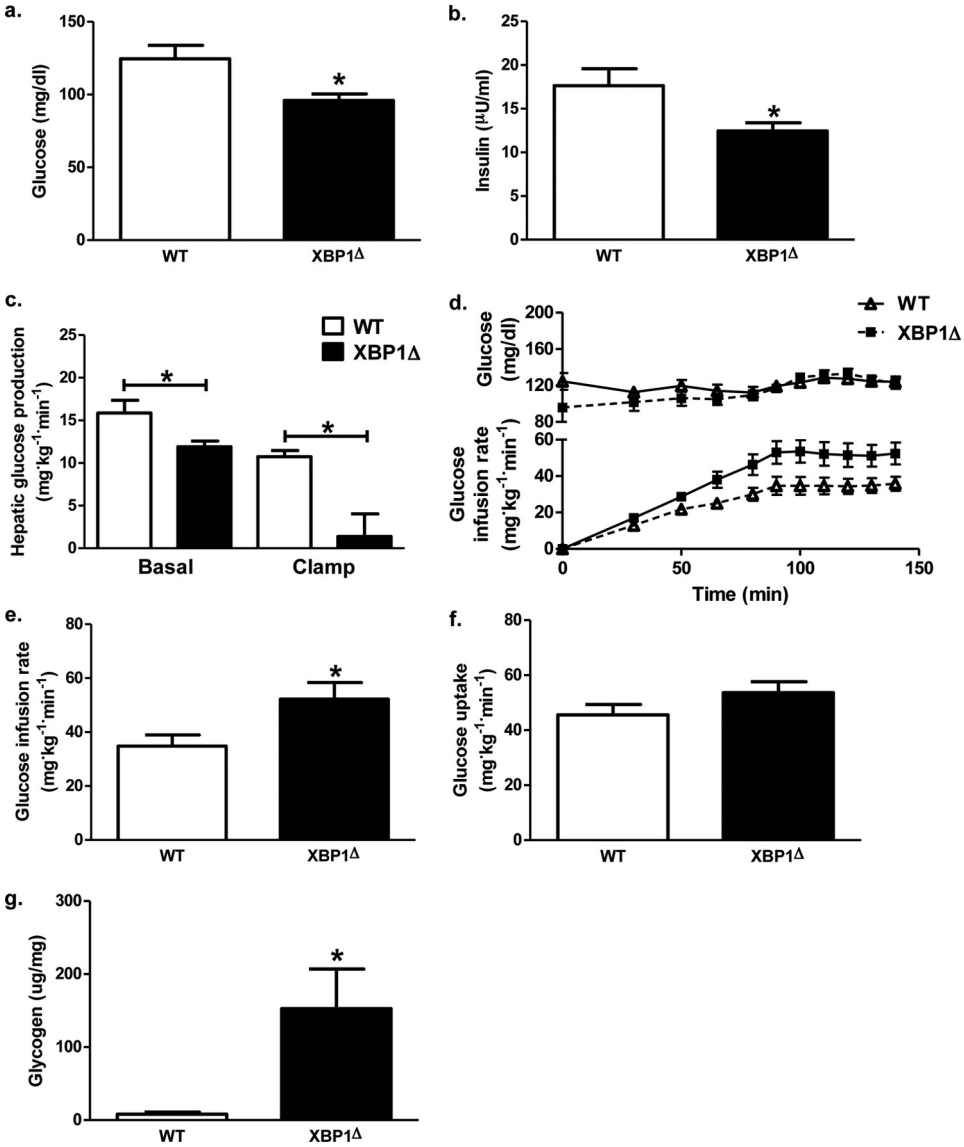

FIGURE 3. **Hepatic insulin sensitivity is improved in fructose chow-fed XBP1Δ mice.** *a*, plasma glucose levels after a 14-h overnight fast. *b*, plasma insulin levels after a 14-h overnight fast. *c*, basal and insulin-stimulated (clamp) hepatic glucose production. *d*, plasma glucose levels (*upper panel*) and glucose infusion rate (*lower panel*) during hyperinsulinemic euglycemic clamps. *e*, glucose infusion rate required to maintain euglycemia during the final 40 min of the clamp. *f*, whole-body glucose uptake measured over the final 40 min of the clamp. *g*, hepatic glycogen levels measured following hyperinsulinemic euglycemic infusion ($n = 6–9$ for both genotypes for each panel). *, $p < 0.05$.

small fraction of total IRS1 (39) and may account for the low levels detected here. Consistent with improved hepatic insulin sensitivity, IRS2 tyrosine phosphorylation was increased 2-fold in XBP1Δ mice (Fig. 4, *a* and *b*). Insulin-induced phosphorylation of FoxO1 results in nuclear exclusion and proteasomal degradation (40) such that changes in FoxO1 protein levels under insulin-stimulated conditions can reflect insulin sensitivity. Accordingly, post-clamp (insulin-treated) hepatic Foxo1 protein levels were 2-fold less in XBP1Δ mice compared with WT, whereas there were no differences in the expression of PEPCK or G6PC mRNA (Fig. 4, *c* and *d*). Lastly, hepatic DAG content is strongly associated with insulin resistance and activation of PKCϵ in liver in both rodents and humans (2, 12, 21–23, 26, 27, 41, 42), and deletion of PKCϵ in liver by antisense oligonucleotide treatment prevents high-fat diet-induced hepatic insulin resistance (41). Consistent with decreased DAG content in liver and improved hepatic insulin sensitivity, PKCϵ activity was reduced by 20% in XBP1Δ mice (Fig. 4*e*). In contrast, hepatic ceramide content was surprisingly increased by ~2-fold in XBP1Δ mice compared with WT mice (Fig. 1*f*), despite the increase in hepatic insulin sensitivity in the XBP1Δ mice (Fig. 3, *d* and *e*).

DISCUSSION

The high-fat fed mouse is a common experimental model for studying the pathogenesis of hepatic insulin resistance. However, both accumulation of intracellular lipid and induction of the ER stress response are present under high-fat feeding conditions, making mechanistic interpretations difficult. Also, the ER is intimately tied to lipid metabolism, and mice deficient in ER stress response genes are susceptible to severe hepatic steatosis (43, 44). These studies highlight both the importance of

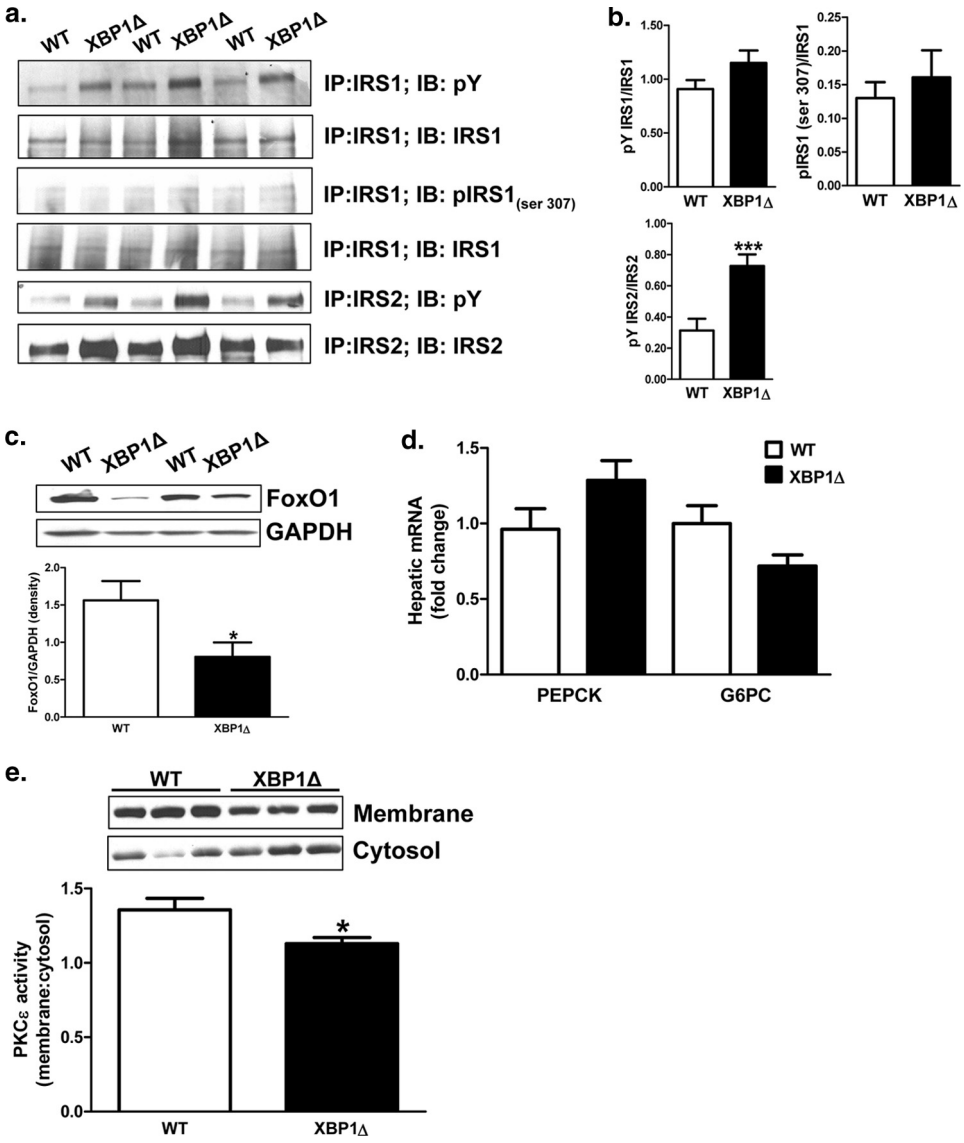

FIGURE 4. **Decreased PKCϵ activity is associated with improved insulin signaling in fructose chow-fed XBP1Δ mice.** *a*, immunoprecipitation of liver lysates from clamped mice for the indicated antibodies, followed by Western blotting. *IP*, immunoprecipitation; *IB*, immunoblot. *b*, quantification of Western blotting data in *A*. *c*, total FoxO1 protein levels in insulin-treated (post-clamp) liver. *d*, hepatic G6PC and PEPCK mRNA levels in insulin-treated (post-clamp) liver determined by QPCR. *e*, PKCϵ activity in post-clamp liver determined as the ratio of membrane to cytosolic levels of PKCϵ. *, $p < 0.05$ ($n = 6$–9 for both genotypes for each panel). The blots shown are representative of six to nine mice per genotype. *, $p < 0.05$.

the ER stress response to the regulation of hepatic lipid metabolism and also the difficulty in interpreting models evaluating both ER stress- and lipid-associated insulin resistance. Here, we describe a novel model where modulation and dissociation of hepatic lipid content and activity of the IRE1α arm of the ER stress response and in turn JNK activity were achieved through genetic and dietary means. We find that despite increased hepatic IRE1α-mediated JNK activity, fructose chow-fed XBP1Δ mice showed increased hepatic insulin sensitivity, which was associated with reduced hepatic DAG content and decreased hepatic PKCϵ activity. In contrast, hepatic ceramide content, which has also been implicated in causing hepatic insulin resistance through inhibition of insulin signaling (4, 45), was ~2-fold higher in the XBP1Δ mice compared with WT mice (Fig. 1*e*), despite increased hepatic insulin sensitivity in the XBP1Δ mice. Taken together, these data demonstrate a central role for the ER in maintaining hepatic lipid homeostasis and suggest that deficits in the ER stress response can result in hepatic insulin resistance indirectly through modulation of hepatic lipogenesis and alterations in hepatic DAG content and PKCϵ activity. Although insulin resistance in skeletal muscle can promote a redistribution of substrates to the liver, resulting in hepatic steatosis and hepatic insulin resistance (46–48), this mechanism cannot explain the observed differences in the XBP1Δ mice, given that there were no differences in insulin-stimulated peripheral glucose uptake between the two groups (Fig. 3*f*).

High-fat diet feeding results in JNK activation in skeletal muscle, adipose, and liver and is associated with insulin resistance (38). Also, JNK-deficient mice are protected from diet-induced obesity and the concomitant development of insulin resistance (38, 49, 50). In contrast, liver-specific deletion of JNK does not protect mice from high-fat diet-induced hepatic insulin resistance (51), supporting the dissociation of hepatic JNK

activity and hepatic insulin resistance observed here. Despite increased hepatic JNK activity in fructose chow-fed XBP1Δ mice, no difference in IRS1 serine 307 phosphorylation was detected, and insulin-stimulated IRS1 tyrosine phosphorylation was modestly improved, although not significantly. Notably, IRS2 tyrosine phosphorylation and degradation of FoxO1 following insulin stimulation were significantly increased in fructose-fed XBP1Δ mice. Phosphorylation of IRS1 at serine 307 is often associated with impaired insulin-stimulated IRS1 tyrosine phosphorylation in insulin resistant models (5, 38). However, IRS1 serine phosphorylation increases with insulin stimulation (39, 52), and IRS1 serine 307 to alanine mutant knock-in mice are not protected from high-fat diet-induced insulin resistance but are paradoxically more susceptible (39). These results and those described here suggest that changes in JNK activity alone cannot account for the observed hepatic insulin resistance in models of high-fat diet feeding and that some other aspect of the high-fat diet condition, such as steatosis or inflammation, is required for the development of hepatic insulin resistance. Also, phosphorylation of IRS1 serine 307 may not play as important a role in the pathogenesis of hepatic insulin resistance as previously thought.

Recently, overexpression of XBP1 was shown to improve glucose homeostasis in models of insulin resistance via a novel interaction with FoxO1 that promoted its proteasomal degradation, in turn reducing gluconeogenic gene expression. This suggests that XBP1 deletion should increase hepatic glucose production under conditions of ER stress (17). Indeed, high-fat fed conditional XBP1 knock-out mice displayed impaired glucose tolerance, although direct quantification of hepatic and peripheral insulin sensitivity was not performed in these studies (17). In contrast, we find that XBP1 deletion, despite increased IRE1α-mediated JNK activation, reduced hepatic glucose production during fructose chow feeding. Dietary selection most likely accounts for the difference, because fructose-induced hepatic steatosis is dependent on hepatic *de novo* lipogenesis, which is deficient in XBP1Δ mice, whereas high-fat feeding is not dependent on *de novo* lipogenesis and results in hepatic lipid accumulation directly by fatty acid oversupply and re-esterification into triglyceride.

Furthermore, we found no difference in the expression of hepatic gluconeogenic genes, despite reduced FoxO1 protein levels following insulin stimulation, which likely reflects increased nuclear exclusion and proteasomal degradation of FoxO1 in XBP1Δ mice because of enhanced insulin signaling compared with the WT control mice. Overexpression of XBP1 may improve glucose homeostasis by improving hepatic steatosis, much in the way pharmacological or genetic enhancement of ER capacity do (6, 7, 53, 54). Although low level expression of XBP1 in ob/ob mice improved glucose homeostasis without apparent changes in XBP1 target gene expression or hepatic insulin sensitivity, lipogenenic XBP1 targets were not reported, and portal infusion of a relatively high insulin dose may have masked subtle changes in insulin sensitivity, which may alternatively explain reductions in FoxO1 protein (17, 40). Lastly, mutation of the XBP1 DNA-binding domain demonstrated that improvements in glucose homeostasis upon XBP1 overexpression do not require transcriptional activity (17). This is an intriguing observation, and although chromatin immunoprecipitation studies suggest that XBP1 can bind directly to promoter regions of lipogenic genes (11), this does not rule out the possibility that XBP1 regulates hepatic lipid metabolism independently of DNA binding.

In summary, we find that despite increased hepatic IRE1α-mediated JNK activation and the presence of classic markers of ER stress, fructose-fed XBP1Δ mice were more insulin-sensitive compared with fructose-fed WT control mice. Improvements in insulin sensitivity could be attributed specifically to improved suppression of hepatic glucose production by insulin, which was associated with decreased hepatic diacylglycerol content and PKCϵ activity. These data suggest that IRE1α-mediated JNK activation alone is insufficient to induce hepatic insulin resistance and support the hypothesis that defects in the ER stress response may alter hepatic insulin sensitivity indirectly through modulation of hepatic lipogenesis and subsequent alterations in hepatic DAG content and PKCϵ activity.

Acknowledgments—We thank Dong Zhang (Yale University), Debbie Jiang (Yale University), and Joao Paulo Camporez (Yale University) for technical assistance with these studies.

REFERENCES

1. Rizza, R. A. (2010) Pathogenesis of fasting and postprandial hyperglycemia in type 2 diabetes: implications for therapy. *Diabetes* **59,** 2697–2707
2. Samuel, V. T., Petersen, K. F., and Shulman, G. I. (2010) Lipid-induced insulin resistance: unravelling the mechanism. *Lancet* **375,** 2267–2277
3. Hotamisligil, G. S. (2010) Endoplasmic reticulum stress and the inflammatory basis of metabolic disease. *Cell* **140,** 900–917
4. Holland, W. L., Miller, R. A., Wang, Z. V., Sun, K., Barth, B. M., Bui, H. H., Davis, K. E., Bikman, B. T., Halberg, N., Rutkowski, J. M., Wade, M. R., Tenorio, V. M., Kuo, M. S., Brozinick, J. T., Zhang, B. B., Birnbaum, M. J., Summers, S. A., and Scherer, P. E. (2011) Receptor-mediated activation of ceramidase activity initiates the pleiotropic actions of adiponectin. *Nat. Med.* **17,** 55–63
5. Ozcan, U., Cao, Q., Yilmaz, E., Lee, A. H., Iwakoshi, N. N., Ozdelen, E., Tuncman, G., Görgün, C., Glimcher, L. H., and Hotamisligil, G. S. (2004) Endoplasmic reticulum stress links obesity, insulin action, and type 2 diabetes. *Science* **306,** 457–461
6. Sreejayan, N., Dong, F., Kandadi, M. R., Yang, X., and Ren, J. (2008) *Obesity (Silver Spring)* **16,** 1331–1337
7. Han, M. S., Chung, K. W., Cheon, H. G., Rhee, S. D., Yoon, C. H., Lee, M. K., Kim, K. W., and Lee, M. S. (2009) Imatinib mesylate reduces endoplasmic reticulum stress and induces remission of diabetes in db/db mice. *Diabetes* **58,** 329–336
8. Lee, A. H., Iwakoshi, N. N., and Glimcher, L. H. (2003) XBP-1 regulates a subset of endoplasmic reticulum resident chaperone genes in the unfolded protein response. *Mol. Cell. Biol.* **23,** 7448–7459
9. Yoshida, H., Matsui, T., Yamamoto, A., Okada, T., and Mori, K. (2001) XBP1 mRNA is induced by ATF6 and spliced by IRE1 in response to ER stress to produce a highly active transcription factor. *Cell* **107,** 881–891
10. Calfon, M., Zeng, H., Urano, F., Till, J. H., Hubbard, S. R., Harding, H. P., Clark, S. G., and Ron, D. (2002) IRE1 couples endoplasmic reticulum load to secretory capacity by processing the XBP-1 mRNA. *Nature* **415,** 92–96
11. Lee, A. H., Scapa, E. F., Cohen, D. E., and Glimcher, L. H. (2008) Regulation of hepatic lipogenesis by the transcription factor XBP1. *Science* **320,** 1492–1496
12. Samuel, V. T., Liu, Z. X., Qu, X., Elder, B. D., Bilz, S., Befroy, D., Romanelli, A. J., and Shulman, G. I. (2004) Mechanism of hepatic insulin resistance in non-alcoholic fatty liver disease. *J. Biol. Chem.* **279,** 32345–32353
13. Jurczak, M. J., Lee, H. Y., Birkenfeld, A. L., Jornayvaz, F. R., Frederick, D. W., Pongratz, R. L., Zhao, X., Moeckel, G. W., Samuel, V. T., Whaley,

J. M., Shulman, G. I., and Kibbey, R. G. (2011) SGLT2 deletion improves glucose homeostasis and preserves pancreatic β-cell function. *Diabetes* **60,** 890–898
14. Yu, C., Chen, Y., Cline, G. W., Zhang, D., Zong, H., Wang, Y., Bergeron, R., Kim, J. K., Cushman, S. W., Cooney, G. J., Atcheson, B., White, M. F., Kraegen, E. W., and Shulman, G. I. (2002) Mechanism by which fatty acids inhibit insulin activation of insulin receptor substrate-1 (IRS-1)-associated phosphatidylinositol 3-kinase activity in muscle. *J. Biol. Chem.* **277,** 50230–50236
15. Ayala, J. E., Samuel, V. T., Morton, G. J., Obici, S., Croniger, C. M., Shulman, G. I., Wasserman, D. H., and McGuinness, O. P. (2010) Standard operating procedures for describing and performing metabolic tests of glucose homeostasis in mice. *Dis. Model Mech.* **3,** 525–534
16. Youn, J. H., and Buchanan, T. A. (1993) Fasting does not impair insulin-stimulated glucose uptake but alters intracellular glucose metabolism in conscious rats. *Diabetes* **42,** 757–763
17. Zhou, Y., Lee, J., Reno, C. M., Sun, C., Park, S. W., Chung, J., Lee, J., Fisher, S. J., White, M. F., Biddinger, S. B., and Ozcan, U. (2011) Regulation of glucose homeostasis through a XBP-1-FoxO1 interaction. *Nat. Med.* **17,** 356–365
18. Choi, C. S., Savage, D. B., Kulkarni, A., Yu, X. X., Liu, Z. X., Morino, K., Kim, S., Distefano, A., Samuel, V. T., Neschen, S., Zhang, D., Wang, A., Zhang, X. M., Kahn, M., Cline, G. W., Pandey, S. K., Geisler, J. G., Bhanot, S., Monia, B. P., and Shulman, G. I. (2007) Suppression of diacylglycerol acyltransferase-2 (DGAT2), but not DGAT1, with antisense oligonucleotides reverses diet-induced hepatic steatosis and insulin resistance. *J. Biol. Chem.* **282,** 22678–22688
19. Choi, C. S., Savage, D. B., Abu-Elheiga, L., Liu, Z. X., Kim, S., Kulkarni, A., Distefano, A., Hwang, Y. J., Reznick, R. M., Codella, R., Zhang, D., Cline, G. W., Wakil, S. J., and Shulman, G. I. (2007) Continuous fat oxidation in acetyl-CoA carboxylase 2 knockout mice increases total energy expenditure, reduces fat mass, and improves insulin sensitivity. *Proc. Natl. Acad. Sci. U.S.A.* **104,** 16480–16485
20. Zhang, D., Liu, Z. X., Choi, C. S., Tian, L., Kibbey, R., Dong, J., Cline, G. W., Wood, P. A., and Shulman, G. I. (2007) Mitochondrial dysfunction due to long-chain Acyl-CoA dehydrogenase deficiency causes hepatic steatosis and hepatic insulin resistance. *Proc. Natl. Acad. Sci. U.S.A.* **104,** 17075–17080
21. Matsuzaka, T., Shimano, H., Yahagi, N., Kato, T., Atsumi, A., Yamamoto, T., Inoue, N., Ishikawa, M., Okada, S., Ishigaki, N., Iwasaki, H., Iwasaki, Y., Karasawa, T., Kumadaki, S., Matsui, T., Sekiya, M., Ohashi, K., Hasty, A. H., Nakagawa, Y., Takahashi, A., Suzuki, H., Yatoh, S., Sone, H., Toyoshima, H., Osuga, J., and Yamada, N. (2007) Crucial role of a long-chain fatty acid elongase, Elovl6, in obesity-induced insulin resistance. *Nat. Med.* **13,** 1193–1202
22. Neschen, S., Morino, K., Hammond, L. E., Zhang, D., Liu, Z. X., Romanelli, A. J., Cline, G. W., Pongratz, R. L., Zhang, X. M., Choi, C. S., Coleman, R. A., and Shulman, G. I. (2005) Prevention of hepatic steatosis and hepatic insulin resistance in mitochondrial acyl-CoA:glycerol-*sn*-3-phosphate acyltransferase 1 knockout mice. *Cell Metab.* **2,** 55–65
23. Savage, D. B., Choi, C. S., Samuel, V. T., Liu, Z. X., Zhang, D., Wang, A., Zhang, X. M., Cline, G. W., Yu, X. X., Geisler, J. G., Bhanot, S., Monia, B. P., and Shulman, G. I. (2006) Reversal of diet-induced hepatic steatosis and hepatic insulin resistance by antisense oligonucleotide inhibitors of acetyl-CoA carboxylases 1 and 2. *J. Clin. Invest.* **116,** 817–824
24. Jornayvaz, F. R., Jurczak, M. J., Lee, H. Y., Birkenfeld, A. L., Frederick, D. W., Zhang, D., Zhang, X. M., Samuel, V. T., and Shulman, G. I. (2010) A high-fat, ketogenic diet causes hepatic insulin resistance in mice, despite increasing energy expenditure and preventing weight gain. *Am. J. Physiol. Endocrinol. Metab.* **299,** E808–E815
25. Lee, H. Y., Choi, C. S., Birkenfeld, A. L., Alves, T. C., Jornayvaz, F. R., Jurczak, M. J., Zhang, D., Woo, D. K., Shadel, G. S., Ladiges, W., Rabinovitch, P. S., Santos, J. H., Petersen, K. F., Samuel, V. T., and Shulman, G. I. (2010) Targeted expression of catalase to mitochondria prevents age-associated reductions in mitochondrial function and insulin resistance. *Cell Metab.* **12,** 668–674
26. Shulman, G. I. (2000) Cellular mechanisms of insulin resistance. *J. Clin. Invest.* **106,** 171–176
27. Erion, D. M., and Shulman, G. I. (2010) Diacylglycerol-mediated insulin resistance. *Nat. Med.* **16,** 400–402
28. Deevska, G. M., Rozenova, K. A., Giltiay, N. V., Chambers, M. A., White, J., Boyanovsky, B. B., Wei, J., Daugherty, A., Smart, E. J., Reid, M. B., Merrill, A. H., Jr., and Nikolova-Karakashian, M. (2009) Acid sphingomyelinase deficiency prevents diet-induced hepatic triacylglycerol accumulation and hyperglycemia in mice. *J. Biol. Chem.* **284,** 8359–8368
29. Urano, F., Wang, X., Bertolotti, A., Zhang, Y., Chung, P., Harding, H. P., and Ron, D. (2000) Coupling of stress in the ER to activation of JNK protein kinases by transmembrane protein kinase IRE1. *Science* **287,** 664–666
30. Ozawa, K., Miyazaki, M., Matsuhisa, M., Takano, K., Nakatani, Y., Hatazaki, M., Tamatani, T., Yamagata, K., Miyagawa, J., Kitao, Y., Hori, O., Yamasaki, Y., and Ogawa, S. (2005) The endoplasmic reticulum chaperone improves insulin resistance in type 2 diabetes. *Diabetes* **54,** 657–663
31. Nakatani, Y., Kaneto, H., Kawamori, D., Yoshiuchi, K., Hatazaki, M., Matsuoka, T. A., Ozawa, K., Ogawa, S., Hori, M., Yamasaki, Y., and Matsuhisa, M. (2005) Involvement of endoplasmic reticulum stress in insulin resistance and diabetes. *J. Biol. Chem.* **280,** 847–851
32. Shaffer, A. L., Shapiro-Shelef, M., Iwakoshi, N. N., Lee, A. H., Qian, S. B., Zhao, H., Yu, X., Yang, L., Tan, B. K., Rosenwald, A., Hurt, E. M., Petroulakis, E., Sonenberg, N., Yewdell, J. W., Calame, K., Glimcher, L. H., and Staudt, L. M. (2004) XBP1, downstream of Blimp-1, expands the secretory apparatus and other organelles, and increases protein synthesis in plasma cell differentiation. *Immunity* **21,** 81–93
33. Acosta-Alvear, D., Zhou, Y., Blais, A., Tsikitis, M., Lents, N. H., Arias, C., Lennon, C. J., Kluger, Y., and Dynlacht, B. D. (2007) XBP1 controls diverse cell type- and condition-specific transcriptional regulatory networks. *Mol. Cell* **27,** 53–66
34. Whitmarsh, A. J., and Davis, R. J. (2001) Analyzing JNK and p38 mitogen-activated protein kinase activity. *Methods Enzymol.* **332,** 319–336
35. Wu, J. J., Roth, R. J., Anderson, E. J., Hong, E. G., Lee, M. K., Choi, C. S., Neufer, P. D., Shulman, G. I., Kim, J. K., and Bennett, A. M. (2006) Mice lacking MAP kinase phosphatase-1 have enhanced MAP kinase activity and resistance to diet-induced obesity. *Cell Metab.* **4,** 61–73
36. Solinas, G., and Karin, M. (2010) JNK1 and IKKβ: molecular links between obesity and metabolic dysfunction. *FASEB J.* **24,** 2596–2611
37. Aguirre, V., Uchida, T., Yenush, L., Davis, R., and White, M. F. (2000) The c-Jun NH_2-terminal kinase promotes insulin resistance during association with insulin receptor substrate-1 and phosphorylation of Ser^{307}. *J. Biol. Chem.* **275,** 9047–9054
38. Hirosumi, J., Tuncman, G., Chang, L., Görgün, C. Z., Uysal, K. T., Maeda, K., Karin, M., and Hotamisligil, G. S. (2002) A central role for JNK in obesity and insulin resistance. *Nature* **420,** 333–336
39. Copps, K. D., Hancer, N. J., Opare-Ado, L., Qiu, W., Walsh, C., and White, M. F. (2010) Irs1 serine 307 promotes insulin sensitivity in mice. *Cell Metab.* **11,** 84–92
40. Matsuzaki, H., Daitoku, H., Hatta, M., Tanaka, K., and Fukamizu, A. (2003) Insulin-induced phosphorylation of FKHR (Foxo1) targets to proteasomal degradation. *Proc. Natl. Acad. Sci. U.S.A.* **100,** 11285–11290
41. Samuel, V. T., Liu, Z. X., Wang, A., Beddow, S. A., Geisler, J. G., Kahn, M., Zhang, X. M., Monia, B. P., Bhanot, S., and Shulman, G. I. (2007) Inhibition of protein kinase Cepsilon prevents hepatic insulin resistance in nonalcoholic fatty liver disease. *J. Clin. Invest.* **117,** 739–745
42. Kumashiro, N., Erion, D. M., Zhang, D., Kahn, M., Beddow, S. A., Chu, X., Still, C. D., Gerhard, G. S., Han, X., Dziura, J., Petersen, K. F., Samuel, V. T., and Shulman, G. I. (2011) Cellular mechanism of insulin resistance in nonalcoholic fatty liver disease. *Proc. Natl. Acad. Sci. U.S.A.* **108,** 16381–16385
43. Rutkowski, D. T., Wu, J., Back, S. H., Callaghan, M. U., Ferris, S. P., Iqbal, J., Clark, R., Miao, H., Hassler, J. R., Fornek, J., Katze, M. G., Hussain, M. M., Song, B., Swathirajan, J., Wang, J., Yau, G. D., and Kaufman, R. J. (2008) UPR pathways combine to prevent hepatic steatosis caused by ER stress-mediated suppression of transcriptional master regulators. *Dev. Cell* **15,** 829–840
44. Yamamoto, K., Takahara, K., Oyadomari, S., Okada, T., Sato, T., Harada, A., and Mori, K. (2010) Induction of liver steatosis and lipid droplet for-

mation in ATF6α-knockout mice burdened with pharmacological endoplasmic reticulum stress. *Mol. Biol. Cell* **21,** 2975–2986
45. Bikman, B. T., and Summers, S. A. (2011) Ceramides as modulators of cellular and whole-body metabolism. *J. Clin. Invest.* **121,** 4222–4230
46. Kim, J. K., Zisman, A., Fillmore, J. J., Peroni, O. D., Kotani, K., Perret, P., Zong, H., Dong, J., Kahn, C. R., Kahn, B. B., and Shulman, G. I. (2001) Glucose toxicity and the development of diabetes in mice with muscle-specific inactivation of GLUT4. *J. Clin. Invest.* **108,** 153–160
47. Kotani, K., Peroni, O. D., Minokoshi, Y., Boss, O., and Kahn, B. B. (2004) GLUT4 glucose transporter deficiency increases hepatic lipid production and peripheral lipid utilization. *J. Clin. Invest.* **114,** 1666–1675
48. Petersen, K. F., Dufour, S., Savage, D. B., Bilz, S., Solomon, G., Yonemitsu, S., Cline, G. W., Befroy, D., Zemany, L., Kahn, B. B., Papademetris, X., Rothman, D. L., and Shulman, G. I. (2007) The role of skeletal muscle insulin resistance in the pathogenesis of the metabolic syndrome. *Proc. Natl. Acad. Sci. U.S.A.* **104,** 12587–12594
49. Sabio, G., Das, M., Mora, A., Zhang, Z., Jun, J. Y., Ko, H. J., Barrett, T., Kim, J. K., and Davis, R. J. (2008) A stress signaling pathway in adipose tissue regulates hepatic insulin resistance. *Science* **322,** 1539–1543
50. Sabio, G., Kennedy, N. J., Cavanagh-Kyros, J., Jung, D. Y., Ko, H. J., Ong, H., Barrett, T., Kim, J. K., and Davis, R. J. (2010) Role of muscle c-Jun NH_2-terminal kinase 1 in obesity-induced insulin resistance. *Mol. Cell. Biol.* **30,** 106–115
51. Sabio, G., Cavanagh-Kyros, J., Ko, H. J., Jung, D. Y., Gray, S., Jun, J. Y., Barrett, T., Mora, A., Kim, J. K., and Davis, R. J. (2009) Prevention of steatosis by hepatic JNK1. *Cell Metab.* **10,** 491–498
52. Um, S. H., Frigerio, F., Watanabe, M., Picard, F., Joaquin, M., Sticker, M., Fumagalli, S., Allegrini, P. R., Kozma, S. C., Auwerx, J., and Thomas, G. (2004) Absence of S6K1 protects against age- and diet-induced obesity while enhancing insulin sensitivity. *Nature* **431,** 200–205
53. Ozcan, U., Yilmaz, E., Ozcan, L., Furuhashi, M., Vaillancourt, E., Smith, R. O., Görgün, C. Z., and Hotamisligil, G. S. (2006) Chemical chaperones reduce ER stress and restore glucose homeostasis in a mouse model of type 2 diabetes. *Science* **313,** 1137–1140
54. Ye, R., Jung, D. Y., Jun, J. Y., Li, J., Luo, S., Ko, H. J., Kim, J. K., and Lee, A. S. (2010) Grp78 heterozygosity promotes adaptive unfolded protein response and attenuates diet-induced obesity and insulin resistance. *Diabetes* **59,** 6–16